

Radionuclide Imaging of Tumor Xenografts in Mice Using a Gelatinase-targeting Peptide

OULA PENATE MEDINA^{1,5}, KALEVI KAIREMO^{1,4,5}, HELI VALTANEN^{1,5}, AINO KANGASNIEMI¹, SAMI KAUKINEN^{1,5}, ILONA AHONEN², PERTTU PERMI², ARTO ANNILA², MIA SNECK¹, JUHA M. HOLOPAINEN³, SIRKKA-LIISA KARONEN⁴, PAAVO K. J. KINNUNEN³ and ERKKI KOIVUNEN¹

¹Department of Biosciences, Division of Biochemistry, University of Helsinki, Viikinkaari 5, Helsinki, FIN-00014;

²NMR Laboratory, Structural Biology and Biophysics, Institute of Biotechnology, P.O. Box 65, Helsinki, FIN-00014;

³Helsinki Biophysics & Biomembrane Group, P.O.Box 63, Biomedicum, Haartmaninkatu 8, Helsinki, FIN-00014;

⁴Department of Clinical Chemistry, University Hospital of Helsinki, Haartmaninkatu, Helsinki, FIN-00014;

⁵CTT Cancer Targeting Technologies, Viikinkaari 4 C, Helsinki, FIN-00790, Finland

Abstract. Tumors express MMP-2 and MMP-9 gelatinases, which are involved in the formation of tumor vasculature. This suggests that a tumor and its surrounding neovasculature can be visualized by a sensitive gelatinase recognition method. We have studied tumor radioimaging using a gelatinase inhibitory peptide CTTHWGFTLC (CTT), which in a mouse model targets the tumor site following an intravenous injection. We determined a solution NMR structure of CTT and its retro-inversion peptide, and prepared ¹²⁵I and ^{99m}Tc-labelled CTT peptide derivatives. Radiolabelled CTT inhibited gelatinases *in vitro*, and homed to a tumor xenograft in mice. In normal mice, CTT was instead rapidly cleared from the circulation mainly through the kidney and, after 24 h, no significant radioactivity was accumulated in healthy tissues. Gamma camera imaging of a primary tumor in live mice was obtained with double-labelled liposomes, which were coated with ^{99m}Tc-CTT and encapsulated with ¹²⁵I-albumin. CTT also targeted liposomes to the lungs of tumor-bearing mice, which may indicate the existence of non-visible lung micrometastases. Our studies suggest that selective

gelatinase-targeting compounds could be useful in the early detection and imaging of primary tumors and metastases.

Early detection of primary tumors and metastases would greatly benefit cancer patients. Many cancers are observed at a time point when they have spread and therapeutic intervention is difficult. Only a few methods are available for early and reliable tumor diagnosis, which can be performed in a larger population. These include mammography for the detection of breast cancer and the PSA test for detection of prostate cancer (1), but unfortunately these techniques are not cancer-specific. Early detection of recurrent and metastatic disease may lead to better prognosis. Therefore, there is a need for general cancer-specific markers, which could be utilized in early tumor detection, localization, grading, staging and follow-up. One example fulfilling some of these tasks is an octapeptide called octreotide, which can be used for early detection, localization and follow-up of both recurrent and metastatic disease, especially in neuroendocrine tumors (2). This peptide, with several different conjugates, already has wide applications in clinical oncology.

Agents that preferentially recognize tumor tissue or are able to home to the tumor vasculature following an intravenous injection could provide a means for accurate tumor imaging. Several antibody conjugates have been examined in tumor therapy and imaging in animal models (3, 4). The *in vivo* phage display application was developed to search for small molecular weight peptides that can gain access to the tumor or other desired tissue from the circulation (5). Peptides recognizing the tumor vasculature (6) or tumor lymphatics (7) have been obtained by screening with random peptide libraries in mice. Recently, the first biopanning was carried out in a human patient with the goal of identifying clinically useful organ-targeting peptides (8).

Abbreviations: BSA, bovine serum albumin; CTT, CTTHWGFTLC; NOESy, nuclear Overhauser enhancement spectroscopy; PSA, prostate specific antigen; RMSD, root mean square deviation; TOCSY, total correlation spectroscopy; HSQC, heteronuclear correlation spectroscopy.

Correspondence to: Prof Kalevi Kairemo, Division of Nuclear Medicine, Department of Oncology, Helsinki University Central Hospital, Haartmaninkatu 4, 00029 Helsinki, Finland. Tel: +358-9-47160892, Fax: +358-9-31936398, e-mail: Kalevi.Kairemo@cancertargeting.com

Key Words: Angiogenesis, imaging, liposomes, matrix metalloproteinases, phage display.

One of the peptides that shows tumor homing ability in the mouse model is CTTHWGFTLC (CTT), a selective inhibitor of MMP-2 and MMP-9 gelatinases (9). When the peptide is given to mice bearing subcutaneous tumors, the peptide can prevent tumor growth and prolong the survival of cancer-bearing mice. Several studies have shown that tumors express elevated levels of MMP-2 and MMP-9 and that the enzymes are produced not only by the tumor cells (10), but also by angiogenic endothelial cells (11), tumor infiltrating leukocytes (12) and the stroma surrounding a tumor (13). Thus, because of their total high expression levels in tumors, gelatinases can be considered potential targets to deliver therapeutic and imaging agents to tumors. A recent study showed that tumor imaging in mouse can be achieved with a sensitive peptide substrate, which, after cleavage by MMP-2, gives a fluorescent label (14). A more controversial issue is whether inhibition of all MMP enzyme activity is an appropriate strategy for cancer therapy. Many clinical trials with MMP inhibitors have failed (15) and, in some animal models, inhibition of MMP-9 can even lead to unwanted results with enhanced tumor angiogenesis and tumor growth due to suppression of angiostatin production (16).

Nevertheless, the documented roles of MMP-2 and MMP-9 in angiogenesis (11) and the elevated expression by tumor cells (10) suggest that selective MMP-2/MMP-9- targeting compounds can reveal tumor sites at the point these start to develop and become dependent on the nurturing vasculature provided by the host. Towards this imaging goal, we have here synthesized derivatives of CTT that can be radiolabelled or bound to isotope-containing liposomes. Because of its amphiphilic properties, being both water-soluble and hydrophobic, CTT readily binds to the surface of liposomes and can be used as a targeting agent to deliver liposomes to gelatinase-expressing cells (17). We studied the biodistribution of these potential tumor-imaging agents in mice bearing tumor xenografts and found the ability of CTT to localize the tumor site in live mice.

Materials and Methods

Reagents. All reagents, unless stated otherwise, were obtained from Sigma-Aldrich (St Louis, Missouri, USA) and culture media from Gibco Life Technologies (Paisley, Scotland).

Synthetic peptides. Peptides were synthesized on an Applied Biosystems 433A (Foster City, CA, USA) automatic synthesizer using Fmoc-chemistry. For disulfide generation, peptides were dissolved at 1 mg/ml in 0.05 M ammonium acetate (pH 8) and mixed with H₂O₂ for 40 min at room temperature so that 0.5 ml of 3 % H₂O₂ was added per 100 mg peptide. The peptides were purified by reversed phase HPLC and the molecular weight was identified by mass spectrometry analysis.

NMR. CTT and retro-inverse peptide samples for NMR spectroscopy were prepared by dissolving freeze-dried peptides in

aqueous buffer to result in approximately 2 mM samples. All spectra were acquired by a Varian Unity Inova 600 MHz NMR spectrometer, equipped with a ¹H/¹³C/¹⁵N triple-resonance probehead with an actively shielded z-axis gradient system. The proton assignments were derived from phase-sensitive two-dimensional TOCSY (18) and NOESY (19) spectra acquired at 2 and 8 °C to adjust the rotational correlation time suitable for NOE experiments. TOCSY spectra were recorded with 30, 75 and 120 ms mixing times using DIPSI-2rc spin-lock (20), whereas NOESY spectra were measured using 300 ms mixing time. The spectra were recorded with 512 and 4512 complex points in F₁ and F₂ dimension, corresponding to acquisition times of 56.9 and 501.3 ms, respectively. In addition one-bond proton carbon correlation spectra, ¹³C-HSQC (21) were taken to ascertain the assignments. Two hundred and fifty-six and 4000 complex points were collected corresponding to 12.1 and 400 ms acquisition times in F₁ and F₂, respectively. Short interproton distance restraints were extracted from two-dimensional NOE spectra and main chain torsion angles HN-H^α scalar couplings from proton spectrum. For the structure generation, refinement and quality assessment we employed DYANA(22).

Cell culture. KS1767 Kaposi's sarcoma and HT 1080 fibrosarcoma cells were maintained in DMEM medium supplemented with 10% fetal bovine serum, Glutamax I, penicillin 100 U/ml and streptomycin 0.1 mg/ml. Cell invasion assay was conducted using Matrigel-coated invasion chambers in the serum-containing medium as described (9).

MMP-2 activity assay. MMP-2 activity was measured using a fluorogenic peptide substrate MCA-Pro-Leu-Ala-Nva-Dpa-Ala-Arg-NH₂ (Calbiochem, San Diego, CA, USA) on a MOS-250 fast reaction spectrofluorometer with a thermostated cuvette compartment (Bio-Logic SA, Claix, France). Excitation was at 330 nm and emission spectra were scanned from 340 to 500 nm. Shortly, 1.1 U of pro-MMP-2 (Roche, Indianapolis, USA) in 60 μl HEPES buffer was activated by 10 mM APMA for 30 min at 37 °C. In each measurement, 1 mU of activated MMP-2 was mixed with 2.5 μM substrate in Hepes buffer in a quartz cuvette of 100 μl volume. Measurements were done at the 0, 2, 4, 6, 8 and 10 min time points. Peptide inhibitors were preincubated for 10 min with MMP-2 before experiment.

Technetium -99m labelling of CTT peptide. One mg of CTT was dissolved in 1 ml of H₂O and kept on cold block. Twenty μl of CTT solution was transferred to a small vial and 50 μg of SnCl₂ was added. After a 15-min incubation, labelling was performed with 8-10 mCi of fresh ^{99m}Tc-technetium (Radioisotope Laboratory of Helsinki University Central Hospital, Finland) for 10 min. The ^{99m}Tc-CTT peptide was purified on a Sep-Pak C18 cartridge (Waters, Milford, MA, USA) using 0.9 % sodium chloride / ethanol (60:40) as the elution solvent. The labelling efficacy was analyzed by ITLC with MEK buffer and was over 95 % after purification.

Iodination of AAY-CTT peptide. The AAY-CTT peptide was labelled with ¹²⁵I using iodogen as a catalyst. 5 MBq of Na¹²⁵I (Amersham, Buckinghamshire, England) in 0.5 ml PBS was added to a tube containing 10 μg dried iodogen and 27 μg AAYCTT-peptide. The mixture was incubated for 20 min at room temperature. The labelled peptide was bound on a Sep-Pak C18 cartridge and eluted with 50% acetonitrile. The solvent was evaporated at +55 °C and the purified

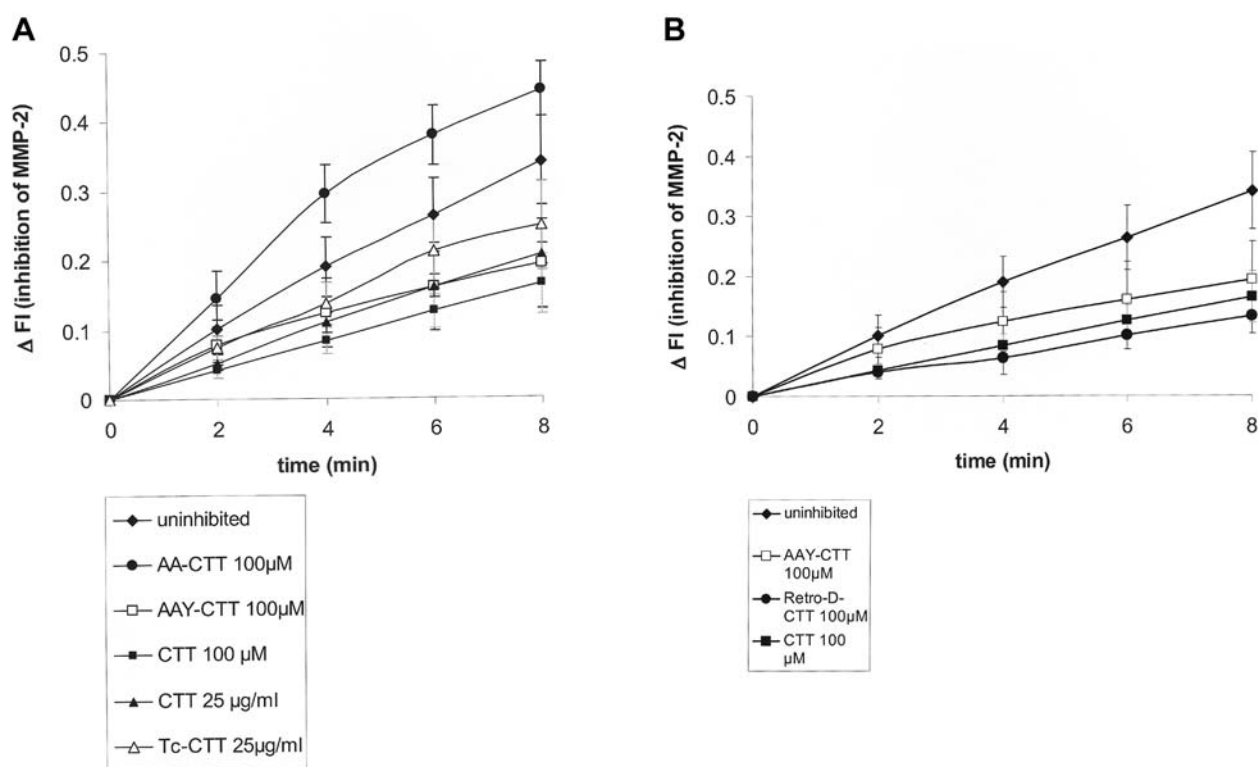


Figure 1. Effect of peptides on MMP-2 activity was determined with a fluorogenic gelatinase substrate. The studied peptides were: /A) AACTT (100 μ M), AAY-CTT (100 μ M), CTT (100 μ M and 25 μ M, 99m Tc-CTT (25 μ M) and B) AAY-CTT (100 μ M), cltfgwhctc (100 μ M), CTT (100 μ M).

dry peptide was then dissolved in 500 μ l of PBS. The activity of the peptide was determined in a gamma counter (Cobra II, Packard Instruments). The AACTT and CTT peptides not containing tyrosine were iodinated by using the N-succinimidyl 3-(tri-n-butylstannyl) benzoate (ATE) method (23)

Preparation of labelled liposomes. Iodination of bovine serum albumin (BSA) was performed by the iodogen 1, 3, 4, 6-tetrachloro-3, 6-diphenylglycoluril method. Briefly, 100 μ l (10 mg/ml) of BSA and 125 I (50MBq) were mixed in a iodogen-coated vial, and 125 I-BSA was then separated from free label on a PD-10 gel filtration column (Pharmacia, Uppsala, Sweden). For encapsulation of 125 I-BSA on liposomes, we used the protocol described earlier for doxorubicin entrapment (17). POPC/POPE lipid stock solutions were mixed in chloroform to obtain the 80:20 mol/mol composition. The solvent was removed under a gentle stream of nitrogen and the lipid residue was subsequently maintained under reduced pressure for at least 2 h. Multilamellar liposomes were formed by hydrating the dry lipids at room temperature with one ml of PBS together with 125 I-BSA so as to yield a lipid concentration of one mM. Multilamellar liposomes were freeze/thawed five times to enhance encapsulation (24). Large unilamellar vesicles were obtained by extruding (25) liposome dispersions 19 times through a 100-nm pore size polycarbonate membrane (Nucleopore, Pleasanton, CA, USA) with a LiposoFast Pneumatic small-volume homogenizer (Avestin, Ottawa, Canada). The pressure used for extrusion of vesicles through the filters was 25 psi (\sim 170 kPa). In some experiments, the 99m Tc-CTT peptide was mixed with the vesicles (17) to bind the peptide on the liposome surface.

Radionuclide imaging of tumor xenografts. Subcutaneous KS1767 Kaposi's sarcoma tumors were made by injecting one million cells per NMRI female nude mouse (Harlan, Netherlands). Tumors usually formed within three weeks.

Approximately 1 – 5 MBq labelled reagent (125 I-AACTT, 125 I-AACTT, 99m Tc-CTT or radioactive liposomes) was injected into avertin-anesthetized mice *via* the tail vein in a volume of 50 μ l - 200 μ l. Gamma imaging was done at 30 min and 24 h following the injection using a Picker Prism 1500XP single-head gamma camera connected to an Odyssey computer (Picker International, Highland Heights, OH, USA). 99m Tc-activity was recorded by using 140 keV energy peak (20% window) and 125 I activity using 30 keV gamma energy peak (35% window). The mice were then sacrificed and blood samples taken for radioactivity measurements. Tumor and other organs were collected and the radioactivity counted. The tumor tissue was sliced to 100- μ m-thick frozen samples using cryotomy and approximately every tenth sample was imaged by autoradiography. The mice were cared for according to the instructions of the animal facility, and the experiments were approved by an ethical committee of Helsinki University, Finland.

Biodistribution of CTT peptide in normal mice. Five anesthetized balb/c mice received a total of 27 μ g 125 I-AACTT peptide (1.05 MBq) *via* tail vein injections. After 30 min, the mice were sacrificed, blood was drawn and tissues were dissected to determine the biodistribution of the peptide. Blood sample, heart, liver, kidneys, lungs, muscle, bone, brain, spleen and thyroid were collected and weighed, and their radioactivity was measured in a gamma counter (Wallac, Turku, Finland).

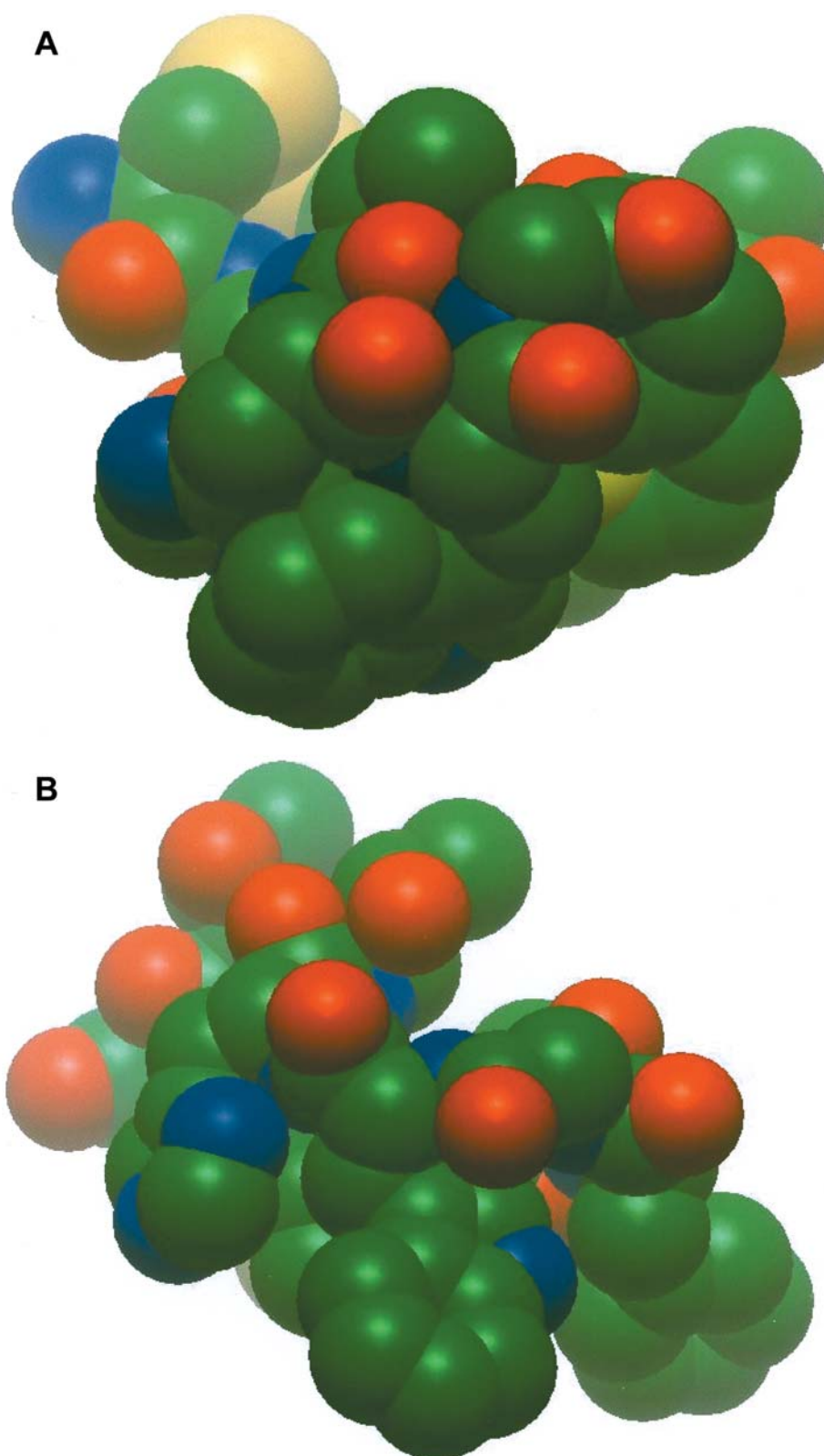


Figure 2. A) Representative solution structure of CTTHWGFTLC peptide and B) an example conformation of [cltfgwhttc] peptide. Short interproton distances and dihedral angle restraints obtained by NMR have been used to obtain the models by restrained torsion angle molecular dynamics. Carbon atoms are shown in green, oxygens in red, nitrogens in blue and sulfur atoms in the disulfides are depicted in yellow.

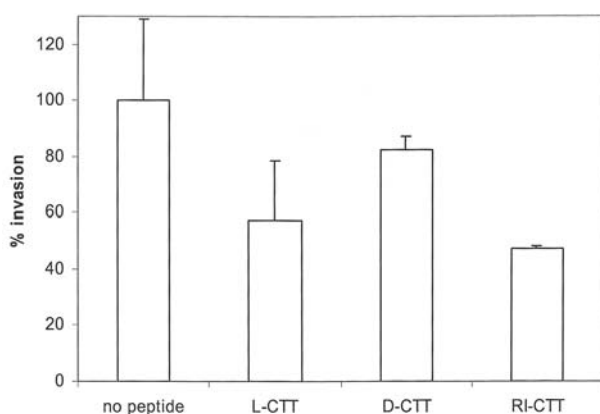


Figure 3. HT1080 cells were plated on Matrigel-coated Transwell filters in the presence or absence of the CTT, cthwgfllc or cltfgwhhcc peptides (each 200 μ M), and allowed to migrate for 18 h. Cells that traversed to the lower site of the filter were stained and the cells were counted on a microscope. The data show mean \pm SD; n=3.

Results

Effect of chemical modification and radiolabelling on the CTT peptide activity. After direct labelling with 125 I on its aromatic residues, the CTT dodecapeptide lost its gelatinase inhibitory activity and could not be used as a tumor-targeting agent in mouse. A tyrosine residue added on the first N-terminal exocyclic position gave a peptide that could be efficiently iodinated without activity loss. The 13 amino acid long 125 I-labelled AAY-CTT peptide inhibited MMP-2 with the same potency as CTT (Figure 1A). MMP-2 activity was assessed with a fluorogenic peptide substrate. The sensitivity of CTT to amino acid modifications is illustrated by the AA-CTT peptide lacking a tyrosine. This peptide was not an inhibitor and surprisingly stimulated the peptide substrate hydrolysis by MMP-2. We also examined peptide labelling with technetium isotope 99m Tc, which can chelate between two cysteine residues(26). The 99m Tc-CTT retained the gelatinase inhibitory activity but was slightly less active than the parent peptide, possibly because of opening of the disulfide bond.

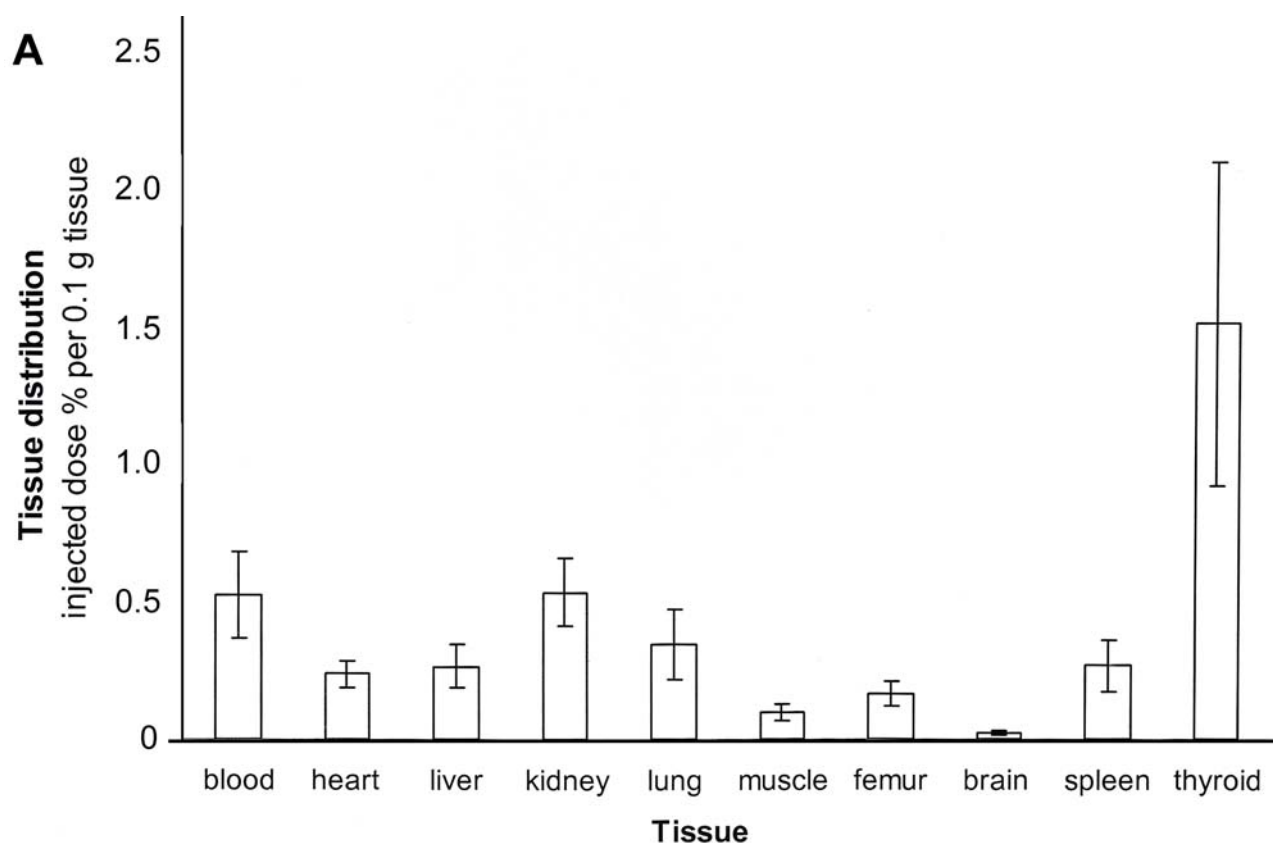
We determined the solution structure for the CTT peptide. It shows that the peptide adopts a well-defined saddle-shaped circular form with RMSD 0.6 ± 0.3 computed from the ten lowest energy structures out of 50 conformers. The side chains, in particular the aromatic His, Trp and Phe residues, approach each other to make a compact structure (Figure 2A), heavy atom RMSD 1.0 ± 0.3 . Iodination of the aromatic residues or increasing the distance between the cysteines can thus be assumed to affect the peptide conformation and cause activity loss. As a retro-inversion peptide can often mimic the structure of the parent peptide (27), we also synthesized the CTT retro-inversion peptide cltfgwhhcc, in which the amino

acids (except the glycine) are in D-form. The NMR structure of cltfgwhhcc has an overall shape similar to that of CTT as expected (Figure 2B). The cltfgwhhcc peptide has protruding side chains, heavy atom RMSD 3.3 ± 1.1 , but the course of the backbone is not as well defined as that of CTT leading to a large dispersion in coordinates RMSD 2.0 ± 0.7 . Though CTT and cltfgwhhcc have structural similarities, the conformations are not identical and this is also indicated by the finding that an antibody made against the CTT peptide (28) did not recognize the cltfgwhhcc peptide in dot blot and microtiter well assays (data not shown).

The cltfgwhhcc retro-inversion peptide had a potent gelatinase-inhibitory activity and inhibited MMP-2 even better than CTT (Figure 1B). Just changing all amino acids to D-form did not generate a gelatinase inhibitor, as the cthwgfllc peptide containing D-amino acids in the original order lacked activity (not shown). In a tumor cell invasion assay, cthwgfllc was also without notable activity, whereas the retro-inversion peptide blocked efficiently, as CTT does (Figure 3).

Biodistribution of radiolabelled CTT peptide in mice. Though the cltfgwhhcc retro-inversion peptide was active, it had a limited water-solubility and was therefore not a good candidate for *in vivo* imaging studies in mice. As indicated above, the iodinated AAY-CTT peptide retained its gelatinase-inhibitory activity and was a safer choice for such experiments. First, the biodistribution of 125 I-labelled AAY-CTT was examined in normal healthy mice following an intravenous injection *via* the tail vein. After a 30-min circulation time, organs were collected to determine peptide homing to different tissues (Figure 4A). Specific CTT peptide accumulation is expected to depend on an expression level of MMP2 and MMP-9. The thyroid accumulated the highest amount of radioactivity. This accumulation is probably due to free 125 I-label released *in vivo* and not to gelatinase binding in the thyroid. Kidney had the next highest amount of radioactivity, suggesting rapid clearance of the peptide by the kidney. Some uptake of the peptide could also be seen in the liver. Overall, the mouse organs accumulated little radioactivity when considering the amount that circulated in the blood. A gram of tissue contained 0.5% or less of the total label injected. When the organs were collected after 24 h, almost all 125 I-CTT had disappeared or metabolized, and the main secretion route was through the kidneys (data not shown).

Next we studied the tumor-homing ability of 125 I-AAY-CTT in mice bearing KS1767 Kaposi's sarcoma xenografts. After an intravenous injection, the peptide achieved a serum concentration of 8.5 – 17 μ M, as calculated on the basis of radioactivity in a blood sample taken. Following a 30-min circulation time, the tumor and its adjacent tissues were sectioned into 100- μ M-thick frozen samples using cryotomy. Approximately every tenth sample was imaged by autoradiography. Figure 4B shows that 125 I-AAY-CTT locates



B AAYCTT

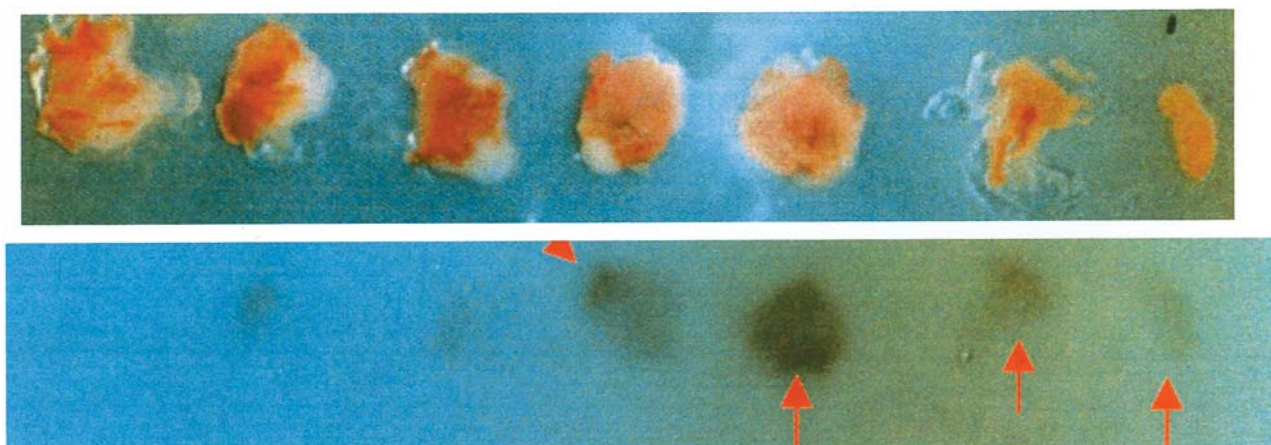
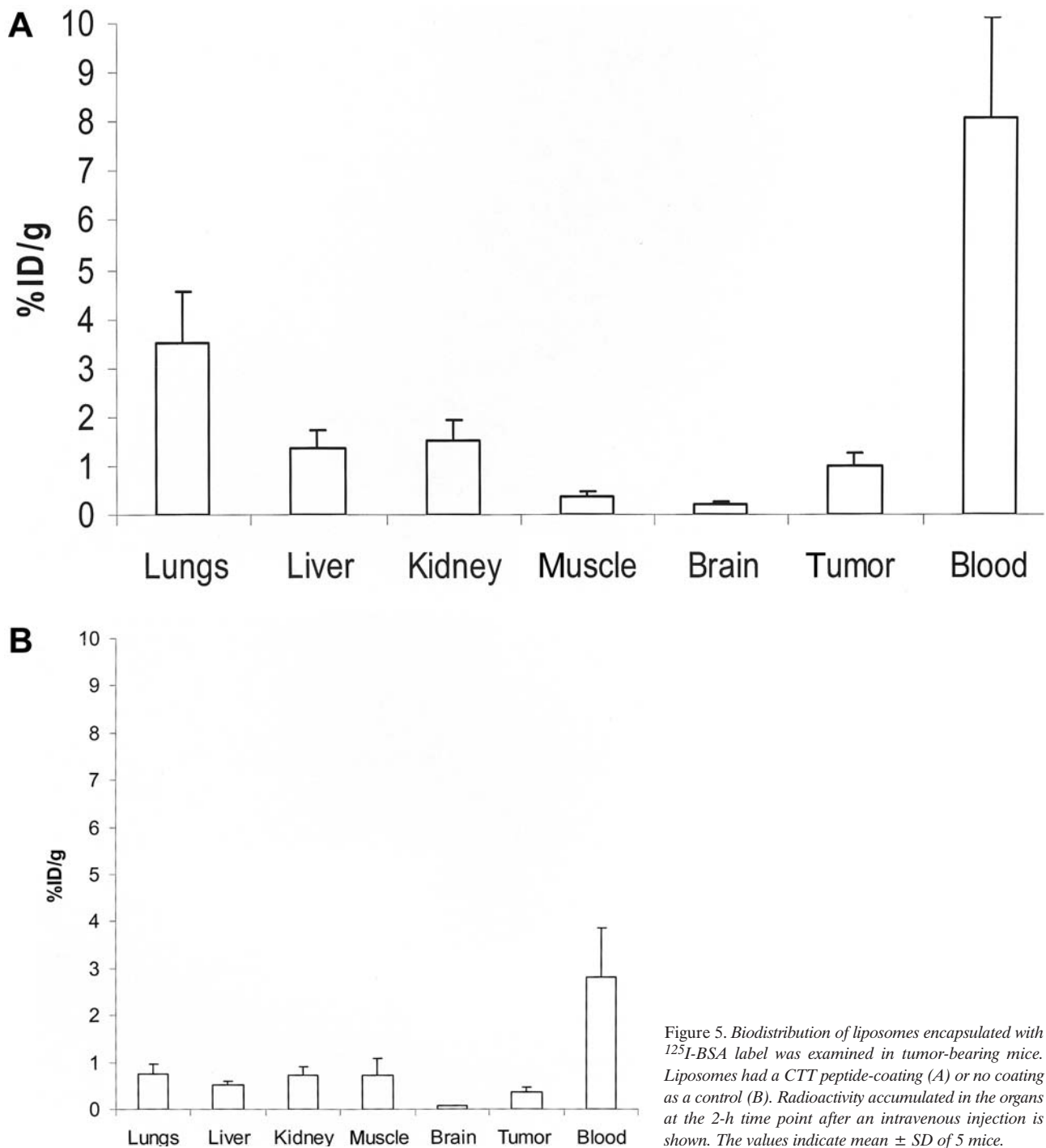


Figure 4. A) Tissue distribution of the ^{125}I -AACTT peptide in normal mice. The biodistribution of the labelled peptide is shown 30 min following injection and was corrected for weight. Results are expressed as percentage of injected dose per 0.1 g tissue (% ID/0.1g). All values are indicated as mean \pm SD of 5 mice. B) Autoradiography of tumor tissue sections of a mouse given ^{125}I -AACTT intravenously. Skin appears right and gluteal muscles left.

in the tumor site but not in the skin (most right) or gluteal muscles (left). As a control, we carried out similar tumor-targeting experiments with ^{125}I -labelled AACTT, in which the labelling abrogated the gelatinase-inhibitory activity. No tumor targeting was seen with ^{125}I -AACTT (not shown).

Tumor imaging with CTT-targeted liposomes. We also examined the suitability of using CTT-coated liposomes for tumor imaging in the mouse model. Liposomes were encapsulated with the ^{125}I -BSA label for easy detection. Uncoated ^{125}I -BSA-containing liposomes were used as a control to see where the



CTT peptide can specifically target the liposomes. The CTT peptide clearly changed the biodistribution of liposomes as studied after 2-h circulation time. As expected, CTT enhanced liposome homing to the primary tumor. Whereas the tumor / muscle-targeting ratio for liposomes in the absence of CTT was 0.5 (Figure 5B), in the presence of CTT it was 2.6 (Figure 5A).

We chose the muscle as the reference tissue, since the muscle is rarely metastasized by tumor, cells. CTT affected liposome binding not only to the tumor but also to apparently normal tissues, where metastases, if present, were not visible. CTT-mediated liposome accumulation was seen particularly in the lungs of tumor-bearing mice. Imaging of the primary tumor in

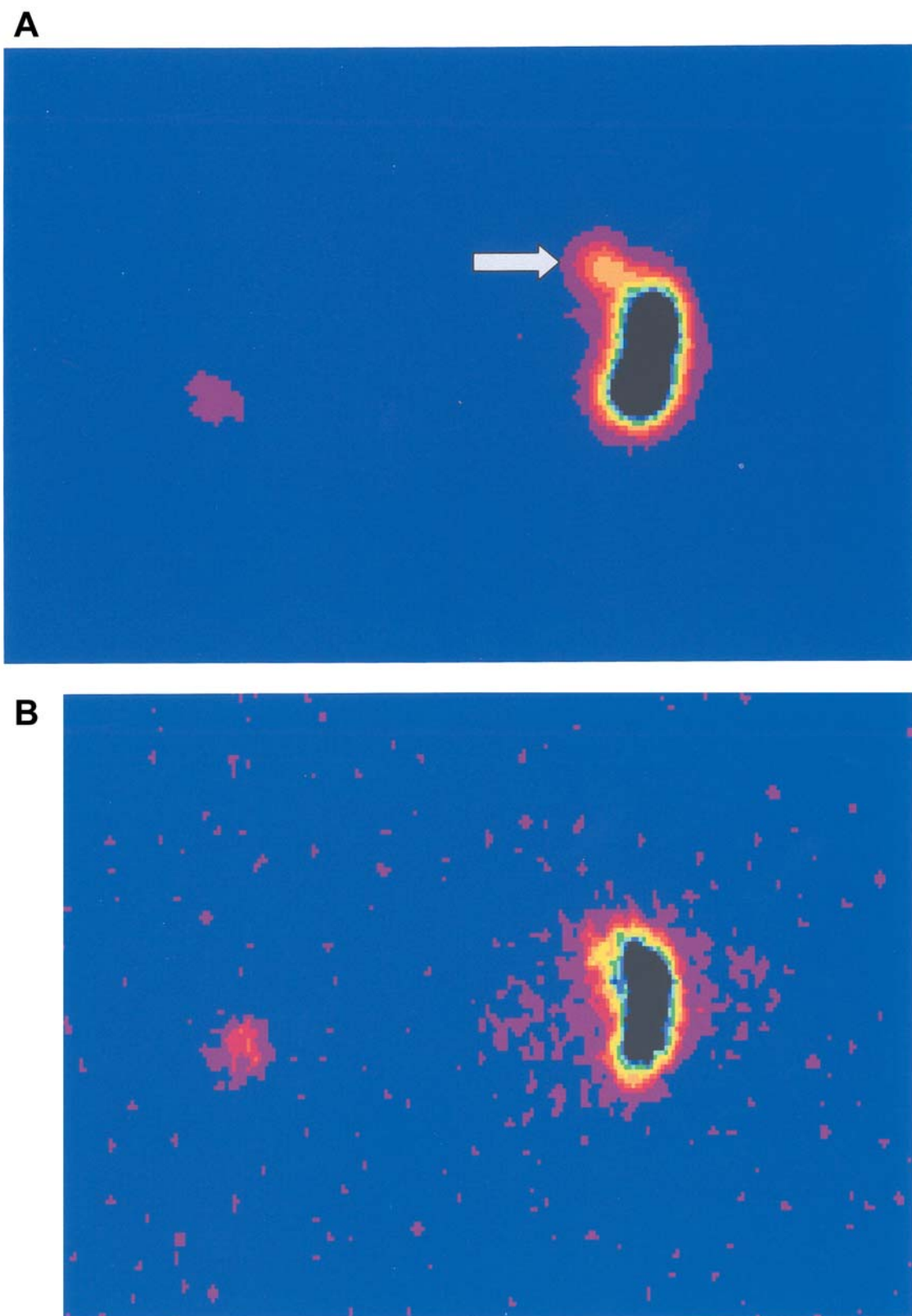


Figure 6. Gamma imaging of live mice with experimental tumors. The figures show examples of animals after 24 h of intravenous injection with ^{99m}Tc -CTT and ^{125}I -BSA double-labelled liposomes (A) or ^{99m}Tc -CTT alone (B). The arrow indicates the tumor site. The injection site in the tail vein is on the left.

live mice was examined by gamma camera. To obtain high liposomal radiolabel intensity, ^{99m}Tc -labelled CTT was used for liposome coating and ^{125}I -labelled BSA for liposome encapsulation. Following a 24-h circulation time, CTT-mediated liposome accumulation in the primary tumor was observed and the tumor site could be visualized (arrow in Figure 6A). During the same time interval, the ^{99m}Tc -CTT peptide alone without liposomes was unable to image the primary tumor (Figure 6B).

Discussion

Our results show the ability of a gelatinase-targeting peptide to localize the tumor site in a mouse model. MMP-2 and MMP-9 gelatinases appear to be a good choice for the purpose of tumor imaging as they are not only expressed by the tumor cells, but also by host cells surrounding the tumor. Particularly, expression by endothelial cells in the neovasculature (10,11,14,15) may significantly contribute to the success of targeting, as the tumor mass itself, which is often necrotic, may be less permeable to exogenous agents and more difficult to image. Earlier studies showed that phage displaying the CTT peptide homes to the tumor xenograft of mouse, indicating that vascular-targeting is indeed possible(9). As radiolabelling of a small molecular weight peptide can easily affect the peptide conformation and activity, we focused our studies on identification of reagents, which are gelatinase inhibitors also after radiolabelling. Two such reagents, ^{125}I -AAAY-CTT and ^{99m}Tc -CTT, were developed and these peptides showed tumor homing ability, either alone or in conjugation with liposomes.

The 3-D structure of the CTT peptide is responsible for its activity, since it has been shown that the linear peptide where cysteines are replaced by serines is inactive. This also makes NMR a powerful tool in controlling the effects of modifications to the overall 3-D structure. Additionally, it shows that there are differences between small peptides with regards to stability of conformation, which is of utmost importance for further conclusions regarding the usefulness of different peptides in clinical studies. This had led to different labelling strategies in various applications of these peptides. Antibodies have been widely used for imaging purposes. Also, peptides that occur naturally have been used for imaging like octreotide. However, there have not been extensive studies where phage display peptide-derived peptides have been used for tumor imaging. In particular, gelatinase-targeting peptide has not been used before.

The NMR studies showed that the CTT peptide adopts a saddle-like structure, which is rigidified by the disulfide bond. The ^{99m}Tc label caused a small decrease in gelatinase inhibitory activity, which may be explained by an increased length between the cysteines due to technetium chelation. We found that ^{99m}Tc -CTT was most effective when coated on the surface of liposomes. This made it possible to image a tumor site by a

gamma camera in a real time. ^{99m}Tc -CTT or liposomes alone did not give a tumor image within a 30-min time-frame, indicating that the combined effect of the two was necessary.

The biodistribution data in healthy and normal mice show that the lifetime of the ^{125}I -AAAY-CTT peptide is relatively short. In 24 h almost all signal is diminished. The main secretion route is through kidneys, but some liver uptake has also been seen. Radioactivity accumulation was seen in the thyroid, apparently due to free iodine released from peptide degradation. Otherwise, the localization of the radiolabelled peptide to the normal tissues investigated was minimal and attributable to blood pool activity. These results suggest that MMP-2 and MMP-9 are not expressed at such high levels in normal tissues as to cause accumulation of the CTT peptide. Circulating blood cells also did not concentrate CTT, and our recent studies show that resting T cells and macrophages extracted from blood do not express gelatinases, with which the CTT peptide would react (Stefanidakis M and Koivunen E, unpublished data). The uptake of hydrophobic and low molecular weight compounds by the liver and the kidney often presents an obstacle for therapy studies. However, the minor accumulation of the AAY-CTT-peptide in normal tissues suggests that it may not cause toxicity problems *in vivo*. This result supports the idea that selective gelatinase-targeting agents could be suitable for diagnostic or therapeutic applications.

CTT-liposomes accumulated also, to some extent, to the lungs in a 2-h time-frame. This is understandable when taking in to consideration the amount of blood flow through the lungs compared with other organs and especially the tumor and muscle tissue. However, it is notable also that in mice-bearing human tumor xenografts, the lungs are principal sites for metastases. Thus, though we did not detect visible lung metastases in the mice, it is possible that CTT-liposomes recognized tiny metastases that were generating. Further experiments are needed to clarify whether metastases can be visualized by a sensitive gelatinase-targeting method.

Liposomes might well be developed into a miniature microscope that can be injected into the circulation to observe abnormal vasculature patterns and tumor formation. The targeting peptide of choice, CTT or another compound, can be linked on the liposome surface by fatty acid tails, hydrophobic peptide anchors, or by direct coupling to phospholipids head groups or polyethylene glycol lipids. Liposomes may have specific lipid, carbohydrate and/or positively-charged coating, which prolongs the liposome circulation time in the blood and causes fewer immunological reactions, but improves the ability to fuse with the target cells. Finally, if the destination is to kill the target cell, liposomes may be encapsulated with doxorubicin (17) or other poison, or a hydrophobic cancer drug can be carried in the lipid bilayer. Our studies describe gelatinase-binding labels that could be starting points towards the goal of accurate imaging and follow-up of tumor development.

Acknowledgements

We thank Mia Johansson and Rabah Soliyamani for their help in peptide preparation and analysis. This study was supported by the Academy of Finland and the Finnish Cancer Society. OM, HV, KK and EK own stocks of the CTT Ltd. company, which also gave support to this research at a later stage.

References

- Duffy MJ: PSA as a marker for prostate cancer. *Ann Clin Biochem* 33: 511-19, 1996.
- Anderson CJ, Dehdashti F, Cutler PD, Schwarz SW, Laforest R, Bass LA, Lewis JS and McCarthy D: W. ⁶⁴Cu-TETA-octreotide as a PET imaging agent for patients with neuroendocrine tumors. *J Nuclear Med* 42: 213-21, 2001.
- Pegram MD and Reese DM: Combined biological therapy of breast cancer using monoclonal antibodies directed against HER2/neu protein and vascular endothelial growth factor. *Seminars Oncol* 29(Suppl. 11): 29-37, 2002.
- Chang SS, Bander NH and Heston WD: Monoclonal antibodies: will they become an integral part of the evaluation and treatment of prostate cancer--focus on prostate-specific membrane antigen? *Curr Opin Urol* 9: 391-95, 1999.
- Pasqualini R and Ruoslahti E: Organ targeting *in vivo* using phage display peptide libraries. *Nature* 380: 364-66, 1996.
- Arap W, Pasqualini R and Ruoslahti E: Cancer treatment by targeted drug delivery to tumor vasculature in a mouse model. *Science* 279: 377-80, 1998.
- Laakkonen P, Porkka K, Hoffman J A and Ruoslahti E: A tumor-homing peptide with a targeting specificity related to lymphatic vessels. *Nat Med* 8: 751-55, 2002.
- Arap W, Kolonin MG, Trepel M, Lahdenranta J, Cardo-Vila M, Giordano RJ, Mintz PJ, Ardeli PU, Yao VJ, Vidal CI, Chen L, Flamm A, Valtanen H, Weavind L M, Hicks ME, Pollock RE, Botz GH, Bucana CD, Koivunen E, Cahill D, Troncoso P, Baggerly KA, Pentz RD, Do KA, Logothetis CJ and Pasqualini R: Steps toward mapping the human vasculature by phage display. *Nat Med* 8: 121-27, 2002.
- Koivunen E, Arap W, Valtanen E, Rainisalo A, Medina OP, Heikkilä P, Kantor C, Gahmberg CG, Salo T, Konttinen YT, Sorsa T, Ruoslahti E and Pasqualini R: Tumor targeting with a selective gelatinase inhibitor *Nat Biotechnol* 17: 768-74, 1999.
- Brooks PC, Stromblad S, Sanders LC, von Schalscha TL, Aimes RT, Stetler-Stevenson WG, Quigley JP and Cheresch DA: Localization of matrix metalloproteinase MMP-2 to the surface of invasive cells by interaction with integrin $\alpha_v\beta_3$. *Cell* 85: 683-93, 1996.
- Nguyen M, Arkell J and Jackson C J: Human endothelial gelatinases and angiogenesis. *Int J Biochem Cell Biol* 33: 960-70, 2001.
- Swallow CJ, Murray MP and Guillem JG: Metastatic colorectal cancer cells induce matrix metalloproteinase release by human monocytes. *Clin Exp Metastasis* 14: 3-11, 1996.
- Saad S, Gottlieb DJ, Bradstock K, Overall CM and Bendall LJ: Cancer cell-associated fibronectin induces release of matrix metalloproteinase-2 from normal fibroblasts *Cancer Res* 62: 283-89, 2002.
- Bremer C, Tung CH and Weissleder R: *In vivo* molecular target assessment of matrix metalloproteinase inhibition. *Nat Med* 7: 743-48, 2001.
- Egeblad M and Werb Z: New functions for the matrix metalloproteinases in cancer progression. *Nat Rev Cancer* 2: 161-74, 2002.
- Pozzi A, LeVine W F and Gardner H: Low plasma levels of matrix metalloproteinase 9 permit increased tumor angiogenesis. *Oncogene* 21: 272-82, 2002.
- Medina OP, Söderlund T, Laakkonen LJ, Tuominen EKJ, Koivunen E and Kinnunen PKJ: Binding of novel peptide inhibitors of type IV collagenases to phospholipid membranes and use in liposome targeting to tumor cells *in vitro*. *Cancer Res* 61: 3978-85, 2001.
- Braunschweiler L and Ernst RR: Coherence transfer by isotropic mixing – application to proton correlation spectroscopy. *J Magn Reson* 53: 521-28, 1983.
- Kumar A, Ernst RR and Wüthrich KA: Two-dimensional nuclear overhauser enhancement (2D NOE) experiment for the elucidation of complete proton-proton cross-relaxation networks in biological macromolecules. *Biochem Biophys Res Commun* 95: 1-6, 1980.
- Cavanagh J and Rance M: Suppression of cross-relaxation effects in TOCSY spectra *via* a modified DIPSI-2 mixing sequence. *J Magn Reson* 96: 670-78, 1992.
- John BK, Plant and Hurd RE: Improved proton-detected heteronuclear correlation using gradient-enhanced z and zz-filters. *J Magn Reson A* 101: 113-17, 1992.
- Günthert P, Mumenthaler C and Wüthrich K: Torsion angle dynamics for NMR structure calculation with the new program DYANA. *J Mol Biol* 273: 283-98, 1997.
- Zalutsky MR, Noska MA, Colapinto EV, Garg PK and Bigner DD: Enhanced tumor localization and *in vivo* stability of a monoclonal antibody radioiodinated using N-succinimidyl 3-(tri-n-butylstannyl)benzoate. *Cancer Res* 49: 5543-49, 1989.
- Clifford CJ, Warren EL, Richard TW and Pfeiffer DR: Factors affecting solute entrapment in phospholipid vesicles prepared by the freeze-thaw extrusion method: a possible general method for improving the efficiency of entrapment. *Chem Phys Lipids* 55: 73-83, 1990.
- MacDonald RC, MacDonald RI, Menco BM, Takeshita K, Subbarao NK and Hu LR: Small-volume extrusion apparatus for preparation of large, unilamellar vesicles. *Biochim Biophys Acta* 1061: 297-303, 1991.
- George AJT, Jamar F, Tai M, Heelan BT, Adams GP, McCartney JE, Houston LL, Weiner LM, Opeprmann H, Peters AM and Huston JS: Radiometal labeling of recombinant proteins by a genetically engineered minimal chelation site: technetium-99m coordination by single-chain Fv antibody fusion proteins through a C-terminal cysteinyl peptide. *Proc Natl Acad Sci* 92: 8358-62, 1995.
- Van Regenmortel MHV and Muller S: D-peptides as immunogens and diagnostic reagents. *Curr Opin Biotechnol* 9: 377-82, 1998.
- Björklund M, Valtanen H, Savilahti H and Koivunen E: Use of intein-directed peptide biosynthesis to improve serum stability and bioactivity of a gelatinase inhibitory peptide. *Comb Chem High Throughput Screen* 6: 29-35, 2003.

Received April 23, 2004

Revised November 2, 2004

Accepted December 1, 2004